Available online at www.sciencedirect.com

SCIENCE DIRECT®

Catalysis Today 110 (2005) 247–254

CATALYSIS TODAY

www.elsevier.com/locate/cattod

Spin design of iron complexes on Fe-ZSM-5 zeolites

A.M. Volodin [a,*], G.M. Zhidomirov [a], K.A. Dubkov [a], E.J.M. Hensen [b], R.A. van Santen [b]

[a] *Boreskov Institute of Catalysis, Siberian Branch of the Russian Academy of Sciences, 630090 Novosibirsk, Russia*
[b] *Schuit Institute of Catalysis, Laboratory of Inorganic Chemistry and Catalysis, Eindhoven University of Technology, The Netherlands*

Abstract

The spin state of iron ions in Fe-ZSM-5 zeolites can be purposefully varied by adsorption of gaseous probe molecules. The resulting Fe complexes with half-integer spin ($S = \frac{1}{2}$, $S = \frac{3}{2}$ and $S = \frac{5}{2}$) can be reliably identified by electron paramagnetic resonance (EPR). A good correlation has been found between the concentration of surface sites active in low-temperature nitrous oxide decomposition and the concentration of low-spin ($S = \frac{1}{2}$) nitrosyl complexes of Fe formed after adsorption of NO molecules. Based on the analysis of the formation of such complexes under varying conditions, we conclude that these active sites contain a binuclear iron complex with $S = 0$ and three adsorbed NO molecules. An approach to investigate various Fe-containing sites in oxidation catalysts is discussed.

Keywords: Fe-ZSM-5; Zeolites; Spin design; Iron complex; Benzene oxidation

1. Introduction

In the last years a large number of publications have been devoted to the investigation of the state of Fe ions accounting for low-temperature N_2O decomposition over iron-containing ZSM-5 zeolites [1–9]. This interest is largely related to the remarkably unusual properties of these materials that are able to selectively convert benzene to phenol using N_2O as oxidant. It has been established that these catalytic properties of Fe-ZSM-5 zeolites are due to the presence of a small amount of sites involving Fe ions. Upon decomposition of nitrous oxide over such sites, often referred to as α-sites, a new form of active oxygen (α-oxygen) is formed that exhibits unusual reactivity [2]. Its interaction with benzene results in selective formation of phenol, even at room temperature, while its reaction with methane yields methanol [10–12]. This catalytic behaviour has led to the proposal that α-oxygen is an analog of active oxygen in methanemonooxygenase enzymes performing biological methane oxidation [11,12]. Mössbauer spectroscopic data has provided strong indications that the active sites are made up of extralattice ferrous ions [12].

Whereas the conventional application of electron paramagnetic resonance (EPR) is limited to the detection of high-spin Fe^{3+} ions ($S = \frac{5}{2}$) and ferromagnetic oxide-like particles and is as such not suitable for the identification of the active sites in iron-containing zeolites [13–15], EPR is one of the most informative spectroscopic techniques for investigation of the structure and properties of low-valence Fe ions in a wide range of enzymes. The interaction with NO molecules leads to the formation of paramagnetic nitrosyl complexes with different spin states which can be identified by characteristic EPR features. As a result, NO is widely used as a spin probe for investigation of the state of Fe^{2+} ions in enzyme systems [16–20]. The application of this method to the characterization of ferrous ions in Fe-containing zeolites has been rather limited [21–23].

In the current paper we report on the possibility of purposeful variation of the spin state of iron various complexes in Fe-ZSM-5 zeolites due to adsorption of gaseous molecules and their investigation by EPR. We will not only discuss the interaction of adsorbed molecules with the various ferrous ions but also study the formation of new complexes formed upon the interaction of oxidizable molecules (H_2, NO, CH_4) with α-oxygen generated upon N_2O decomposition.

2. Experimental

Iron-containing ZSM-5 zeolite similar to the one characterized in detail earlier [15] was prepared by impregnation of the hydrogen form of ZSM-5 zeolite with a $FeCl_3$ solution followed

---

* Corresponding author.
E-mail address: volodin@catalysis.nsk.su (A.M. Volodin).

0920-5861/$ – see front matter © 2005 Elsevier B.V. All rights reserved.
doi:10.1016/j.cattod.2005.09.025

by calcination in vacuum at 773 K for 1 h followed by calcination in oxygen for 1 h. The resulting zeolite contains 1.66 wt.% Al and 0.3 wt.% Fe.

Most experiments have been performed using an in situ EPR apparatus as described in detail elsewhere [15,24]. Homemade computer package EPR–CAD was used for processing of the experimental EPR spectra. The concentrations of paramagnetic species were determined by traditional double integration of the experimental EPR spectra with zero line correction.

Prior to recording spectra, the zeolites were placed in quartz ampoules connected to a vacuum system and subjected to a calcination and vacuum pretreatment at 823 K for dehydration and removal of chemisorbed molecules. The total duration of the oxygen–vacuum treatments prior to the experiments was 6–8 h. In all cases, treatment in oxygen (1 Torr) was carried out with freezing of gaseous reaction products (H_2O, CO_2, etc.) in a trap cooled with liquid nitrogen. The last step consisted of oxidation in molecular oxygen (1 Torr) at 823 K for 1 h. Subsequently, the catalyst was cooled to room temperature in oxygen atmosphere followed by evacuation. After the experiments the initial state of the sample was regenerated using the above procedure. The amounts of adsorbed gases, decomposed N_2O and oxygen thermally desorbed during heating were determined under "in situ" conditions by measuring pressure in he reaction chamber using a Pirani manometer for pressures 10^{-5} to 0.5 Torr and a Mechanotron manometer for pressures from 0.2 to 100 Torr. More precise determination of the concentrations of α-sites was carried out by N_2O decomposition in static vacuum installation as previously described [10–12,32]. Partial gas pressures were determined using a PPT Residual Gas Analyser (MKS Instruments) mass spectrometer and Baratron (MKS Instruments) manometer with linear range from 2×10^{-3} to 2 Torr.

The α-site density was determined from the amount of N_2 released during N_2O decomposition at 473 K. This value was compared with the total amount of oxygen desorbed from the sample after heating to 773 K and the average of these two values was taken.

3. Results and discussion

Ferric ions are usually paramagnetic both in the isolated state and in polynuclear structures. The spin Hamiltonian is usually applied for analysis of the EPR spectra of paramagnetic Fe complexes

$$H = g_0\beta BS + D(S_z^2 - S(S+1)/3) + E(S_x^2 - S_y^2), \qquad (1)$$

where S is the system electron spin and the parameters D and E characterize the axial and rhombic components of the zero-field splitting. The experimental spectra of polyoriented systems yield information about the full spin (S) and the axial symmetry distortion degree (E/D). For Fe-ZSM-5 materials only high-spin ($S = \frac{5}{2}$) states of Fe^{3+} ions have been reliably identified by EPR. Two types of signals are observed: (i) complexes of low symmetry with $g_{\mathrm{eff}} = 4.3$, $E/D = 1/3$ and (ii) octahedral complexes with axial symmetry and tetragonal distortion ($g_\perp = 6.0$, $E/D \ll 1$) [13–15]. Most works also report the presence of wide ferromagnetic resonance signals ($\Delta H > 500$ G) that are related to the presence of residual oxide or oxide-like phases in the zeolites.

3.1. Dehydration and dehydroxylation of Fe-ZSM-5 zeolites

Under conventional storage conditions zeolites contact with air and are consequently extensively hydrated. This leads to significant changes in the state and reactivity of Fe species. Moreover, prior to catalytic reactions these materials are usually dehydrated. Consequently, zeolite activation is essential before EPR or other spectroscopies. Thus, we attempt to follow changes in the state of iron during dehydration.

A typical EPR spectrum of Fe-ZSM-5 after storage in air is presented in Fig. 1. It contains a component with $g = 4.3$ related to isolated Fe^{3+} ions, a wide ferromagnetic resonance (FMR) spectrum and weak components near g_e related to an impurity of Mn^{2+} ions that are hardly noticeable in the background of the wide FMR spectrum. Such spectra are fairly typical for various oxide systems containing Fe impurities or intentionally added Fe species registered in air. Brief evacuation at 293 K does not lead to changes in the spectra. However, prolonged evacuation at room temperature results in almost complete disappearance of the features due to Mn^{2+} ions and significant intensification of the line with $g = 4.3$. An increase of dehydration temperature

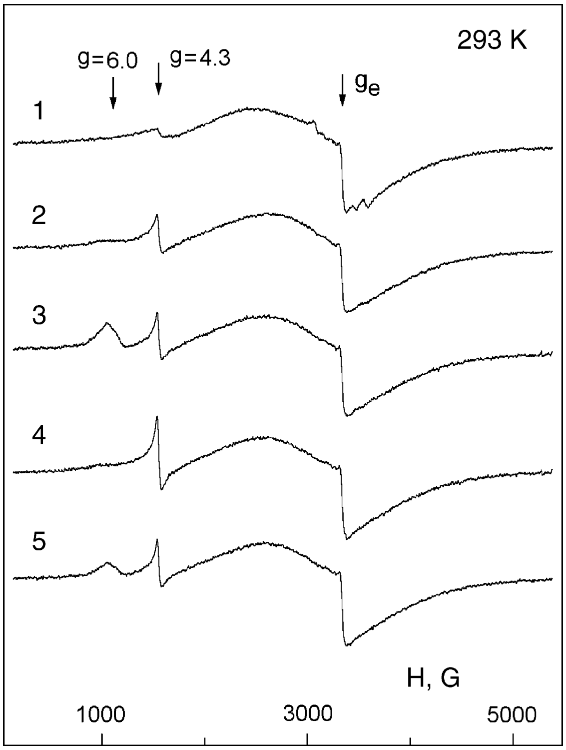

Fig. 1. Evolution of EPR spectra of Fe-ZSM-5 zeolite during dehydration: initial spectrum in ambient air (1), after sample evacuation at room temperature for 12 h (2), after additional dehydration for 1 h at 473 K (3) and 773 K (4) and after sample rehydration at 473 K followed by evacuation at the same temperature (5).

to 473 K leads to the appearance of an intense band with $g_{\perp} = 6$. Further dehydration at 773 K leads to almost complete disappearance of the latter complexes and slight growth in the intensity of the signal with $g = 4.3$. This last step represents the typical last step of zeolite pretreatment prior to low-temperature N_2O decomposition which leads to the stabilization of α-oxygen (O_{α}). All changes in the EPR spectra described above are related to removal of coordinated water and are reversible. Subsequent rehydration of the zeolite at 473 K practically restores its initial state at this temperature.

3.2. Formation of α-oxygen

As noted earlier [15], the formation of α-oxygen was not accompanied by any changes in the EPR spectra. This observation is extremely important for understanding the elementary steps taking place during formation of the active oxygen species. Therefore, we will analyze the formation of these species in more detail.

Quantitative experiments on the formation of α-oxygen were carried out under in situ conditions. The starting point of these experiments was registration of the spectrum of the zeolite, that was activated in vacuum at 793 K, subsequently cooled to 523 K in oxygen and finally evacuated. At this temperature the zeolite was exposed to nitrous oxide which led to the following reaction:

$$N_2O + (\,)_{\alpha} \rightarrow (O)_{\alpha} + N_2 \tag{2}$$

For the present Fe-ZSM-5 zeolite the concentration of O_{α} stabilized on the surface was approximately 1.5×10^{19} sites/g. After deposition of α-oxygen, we did not observe any changes in the intensity or shape of the EPR signal of Fe^{3+} ions with $g = 4.3$ nor the appearance of new lines in the range of the magnetic field from 100 to 6000 G, which corresponds to effective g-values ranging from 1.1 to 30. As neither the sample position in the spectrometer cavity nor it's temperature changed, we conclude that the EPR spectra of this system before and after reaction are absolutely identical. The relative error in determination of the EPR signal intensity under these conditions did not exceed 1%. A similar result was obtained when the EPR spectra were registered at 113 K. To this end, the spectrum of the initial dehydrated zeolite was also recorded at 113 K. Then, the sample was heated to 523 K followed by exposure to nitrous oxide. Subsequently, the sample was cooled to 113 K and its EPR spectrum was registered. Similar experiments were also performed in sealed ampoules. The goal was to compare EPR spectra before and after reaction using low registration temperatures (10–77 K) that are not available in our in situ setup. Also for this case essentially no difference was observe in EPR spectra of zeolites before and after formation of α-oxygen.

Thus, the aggregate of the experimental EPR data obtained in a very wide registration temperature range learns that neither the initial state of the active site nor its state after the α-oxygen formation can be observed by EPR. These results are in good agreement with the data obtained earlier by Mössbauer spectroscopy. These data indicate that Fe^{2+} ions are the active sites in the initial zeolite, and they are oxidized to Fe^{3+} ions during the α-oxygen formation [12]. Hence, we may rewrite reaction (2) as

$$Fe^{2+} + N_2O \rightarrow [Fe^{3+}O^{-}] + N_2 \tag{3}$$

We note here the importance of cooling the sample from the high evacuation temperature to the temperature of nitrous oxide exposure in molecular oxygen to prevent the presence of Fe^{2+} species that do not form α-sites.

These ferrous ions have integer electron spin ($S = 2$) and are consequently not observed in EPR spectra. Fe^{3+} ions in $[Fe^{3+}O^{-}]$ complexes formed after the α-oxygen formation have a high-spin state ($S_1 = \frac{5}{2}$) whereas the α-oxygen ligand is an O^{-} radical anion ($S_2 = \frac{1}{2}$). The aggregate spin of this complex is still integer ($S = 2$, for the most likely case of antiferromagnetic coupling) [25]. In principle, the resulting complex is not amenable to observation by EPR. The possible formation $[Fe^{4+}O^{2-}]$ that is discussed in the literature [26] requires further experimental and theoretical proof and will not be discussed by us. In our opinion, O^{-} radical anions stabilized in the first coordination sphere of Fe^{3+} ions are the most likely candidates for the role of α-oxygen in Fe-ZSM-5 zeolites. Such anion-radicals (or rather $[M^{n+}–O^{-}]$ complexes stabilized on diamagnetic low-coordinated metal cations) are well known on the surface of various oxide catalysts. Usually, they are either observed by EPR themselves or made visible using a proper test reaction [27,28]. The main specific feature of O^{-} radical anions on Fe-ZSM-5 zeolites is their stabilization on paramagnetic Fe^{3+} ions. As a result, the aggregate spin state of such complex determined by the interaction of two paramagnetic fragments is very different from that of O^{-} radical anions on diamagnetic ions (Mg^{2+}, Zn^{2+}, V^{5+}, etc.). As O^{-} radical anions are very reactive towards oxidizable molecules at temperatures as low as 77 K [29–31], we choose such species to convert them into diamagnetic species stabilized on the same Fe^{3+} ions. Reactions with hydrogen and methane appeared to the most suitable.

3.3. Reactions of α-oxygen with H_2 and CH_4

The formation of O^{-} radical anions after N_2O decomposition on reduced surface sites of oxides is due to electron transfer to the adsorbed N_2O molecule followed by its dissociation according to reaction (4) similar to the above reaction describing the formation of α-oxygen [27,28]

$$M^{(n-1)+} + N_2O \rightarrow [M^{n+}O^{-}] + N_2. \tag{4}$$

One of the most typical reactions of oxygen radical anions is hydrogen abstraction from various molecules containing hydrogen atoms

$$[M^{n+}O^{-}] + RH \rightarrow [M^{n+}OH^{-}] + R^{\bullet}. \tag{5}$$

In particular, they easily react with hydrogen and methane as follows:

$$[M^{n+}O^{-}] + H_2 \rightarrow [M^{n+}OH^{-}] + H^{\bullet}, \tag{5a}$$

$$[M^{n+}O^{-}] + CH_4 \rightarrow [M^{n+}OH^{-}] + CH_3^{\bullet}. \tag{5b}$$

The resulting $H^{\bullet}$ and $CH_3^{\bullet}$ radicals are highly reactive and very mobile and are most likely readily engaged in secondary chemical reactions. At low temperatures methyl radicals in some cases can be stabilized on the oxide surface. Such radicals can be registered by EPR [31]. It is noteworthy that these reactions alter the spin of the paramagnetic complex $[M^{n+}O^{-}]$ due to addition of $H^{\bullet}$ radical having its own spin. So, for diamagnetic M^{n+} ions the resulting complexes with hydroxyl groups are not observed by EPR. Mössbauer spectroscopy data [12] have also shown that the α-oxygen atoms in Fe-ZSM-5 exposed to nitrous oxide are of radical anionic nature. They react with hydrogen and methane at temperatures as low at 173 K. The associated activation energies are low [32] and comparable with the activation energies of similar reactions with participation of O^{-} radical anions [30].

Hence, we investigated the reaction of α-oxygen with hydrogen and methane by in situ EPR. In these experiments α-oxygen was formed by N_2O decomposition at 523 K (reaction (2)) followed by evacuation and cooling to the desired reaction temperature (100–250 K). At this temperature hydrogen (or methane) was adsorbed and the kinetics of the formation of new paramagnetic products was monitored. After the experiments the standard state of the zeolite was regenerated by pretreatment at 823 K. We stress that the interaction of the zeolite without α-oxygen with hydrogen or methane does not lead to any changes in its EPR spectra (Fig. 2a).

Fig. 2a and b presents the EPR spectra of the interaction of α-oxygen with hydrogen at 113 K. The reaction results in the appearance of a component with $g_{\perp} = 6$ typical for high-spin ($S = \frac{5}{2}$, $E/D \ll 1$) iron complexes. The second weak component of this spectrum $g_{\parallel} \cong g_e$ is not observed under our conditions. Computer simulation of the spectrum with $g_{\perp} = 6$ and $g_{\parallel} = g_e$ (Fig. 2b) yields a spectrum that is in a very good agreement with the experimental results. Similar complexes were observed during investigation of the zeolite dehydration (Fig. 1). Thus, the obtained results allow us to conclude that reaction with hydrogen is accompanied by a change of the spin state of Fe complexes. This reaction appears to be very similar to the above reactions with the participation of O^{-} radical anions

$$[Fe^{3+}O^{-}] + H_2 \rightarrow [Fe^{3+}OH^{-}] + H^{\bullet}. \qquad (6a)$$

Similar paramagnetic complexes with $g_{\perp} = 6$ and $g_{\parallel} = g_e$ have been also observed during α-oxygen reaction with methane (Fig. 3) that can be described by the following reaction:

$$[Fe^{3+}O^{-}] + CH_4 \rightarrow [Fe^{3+}OH^{-}] + CH_3^{\bullet}. \qquad (6b)$$

The latter two reactions result in the change of the spin state of the iron complexes from $S = 2$ (integer spin, no EPR signal) to $S = \frac{5}{2}$ (half-integer spin, high-spin complexes observed by EPR). These results are in a good agreement with the data obtained for the same reactions by kinetic methods [32,33]. They convincingly show the analogy in the formation and chemical properties of α-oxygen and O^{-} radical anions stabilized on oxide surfaces.

Regeneration of the initial state of the zeolite after reaction with hydrogen or methane requires zeolite dehydroxylation at

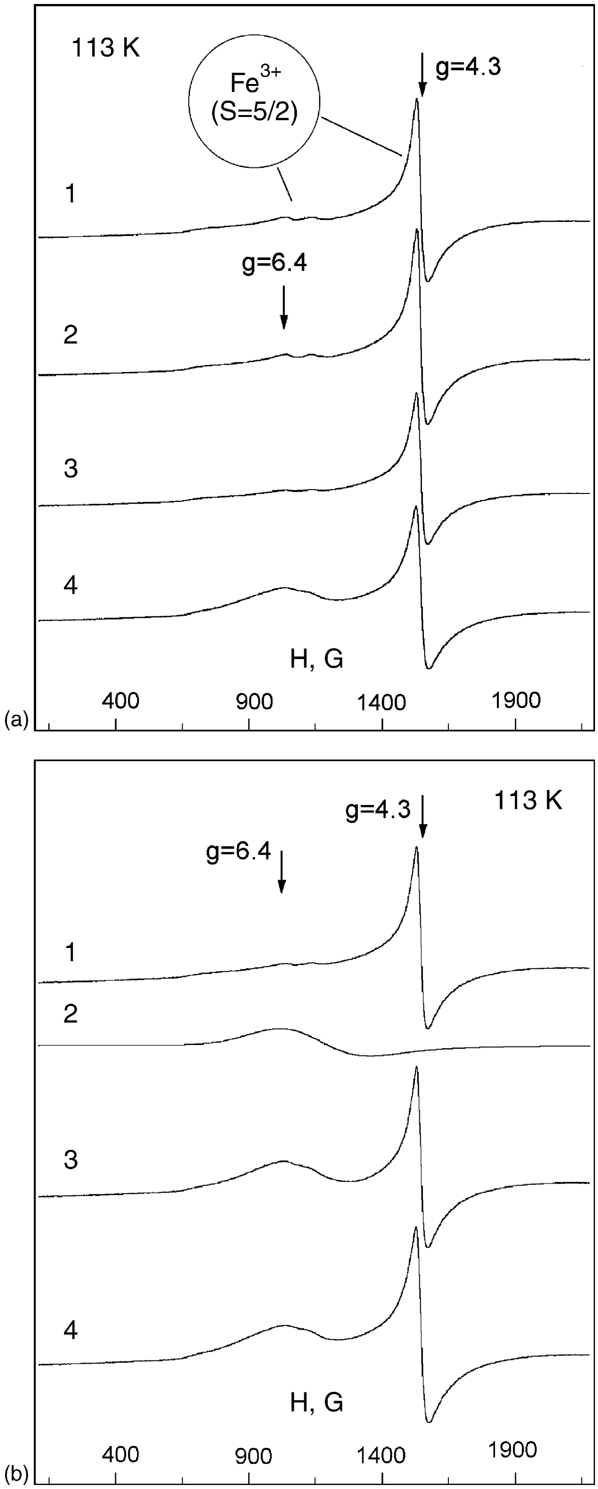

Fig. 2. Reaction of α-oxygen with hydrogen at 113 K: (a) low-field region of the EPR spectra (1) after zeolite activation under vacuum at 773 K, (2) H_2 adsorption (P = 0.2 Torr) at 113 K, (3) α-oxygen formation and (4) reaction of α-oxygen with H_2; (b) low-field region of the EPR spectra (1) after α-oxygen formation, (2) simulated component of the signal with $g_{\perp} = 6.0$, $g_{\parallel} = g_e$ and (3) their sum (spectrum 3 = spectrum 1 + spectrum 2) and (4) the spectrum after α-oxygen reaction with H_2.

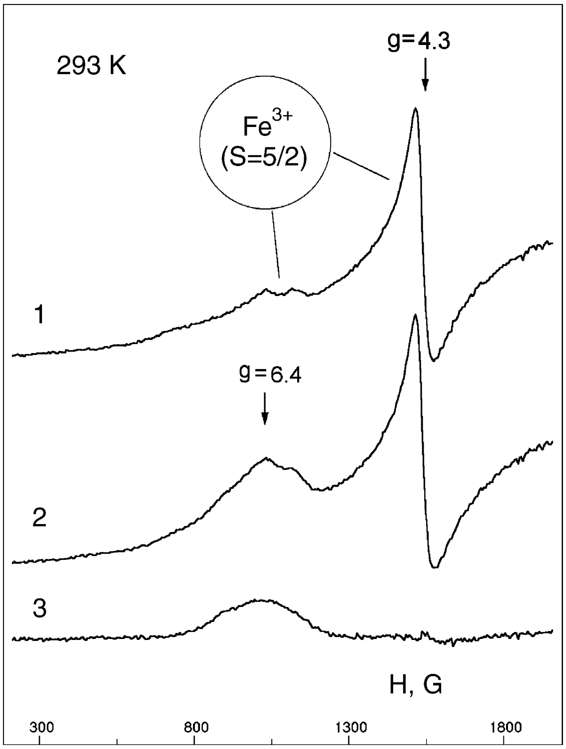

Fig. 3. Methane reaction with α-oxygen at 293 K: the low-field region of the EPR spectra (1) after α-oxygen formation, (2) after its reaction with methane and (3) the difference spectrum.

high temperature. For example, the initial state is completely recovered after the standard oxygen–vacuum treatment at 773 K for 1 h. Moreover, the conditions required for regeneration of the zeolite active sites after its prolonged contact with ambient air and after reaction with hydrogen or methane are similar. The magnetic resonance parameters of the hydroxyl-containing complexes of Fe ions are also identical in both cases ($g_{\perp} = 6$, $g_{\parallel} \cong g_e$). The concentrations of these complexes obtained by two very different pretreatment methods are also close to each other. These results prove that the same hydroxyl-containing high-spin Fe complexes are observed in both cases. High-temperature vacuum treatment in both cases yields high-spin ($S = 2$) Fe^{2+} ions that appear to be sites active in α-oxygen formation. The appearance of such low-valence ions after the zeolite dehydroxylation is described by reaction (7) and is similar to the one suggested in [34]

$$2[Fe^{3+}OH^-] \rightarrow 2[Fe^{2+}] + H_2O + 1/2\,O_2. \qquad (7)$$

Deactivation of the zeolite active sites in ambient air is described by the reverse reaction. This reverse reaction describes deactivation (hydroxylation) of the active sites with water in oxygen-containing atmosphere. The same high-spin hydroxyl complexes of Fe^{3+} can be prepared by the formation of α-oxygen followed by its reaction with hydrogen

$$[Fe^{2+}] + 2N_2O + H_2 \rightarrow 2[Fe^{3+}OH^-] + 2N_2. \qquad (8)$$

The reverse reaction of reaction (7) and reaction (8) involve the same active sites (high-spin Fe^{2+} ions) and result in the formation of the same products (paramagnetic $[Fe^{3+}OH^-]$ complexes). The main and fundamental difference of these reactions is that they use different sources of oxygen and hydrogen for the formation of hydroxyls and hence they take place under different reaction conditions.

3.4. NO interaction with the zeolite active sites

Another approach to alter the spin state of ferrous ions and reveal them by EPR spectroscopy is their reaction with paramagnetic NO molecules adsorbed from the gas phase. As Fe-ZSM-5 zeolites typically contain different ferrous complexes, their reactions with NO should also yield different paramagnetic products.

3.4.1. Fe-nitrosyl complexes with intermediate spin ($S = \frac{3}{2}$)

Fig. 4 presents the EPR spectra obtained after NO adsorption at 173 K on the material dehydrated at 723 K (spectrum 1) and 823 K (spectrum 2). In addition to the signal with $g = 4.3$, spectrum 1 contains components with $g = 6.3$ and $g = 5.7$. When the spectra are registered at temperatures above 77 K, these components are broadened and merge into one component with $g_{\perp} = 6.0$ (Figs. 1–3). It has been noted above that this component is typical for high-spin ($S = \frac{5}{2}$) octahedral complexes of Fe^{3+} ions with strong tetrahedral distortion. EPR spectra with axial symmetry are described by $g_{\perp} = 6$, $g_{\parallel} \cong g_e$.

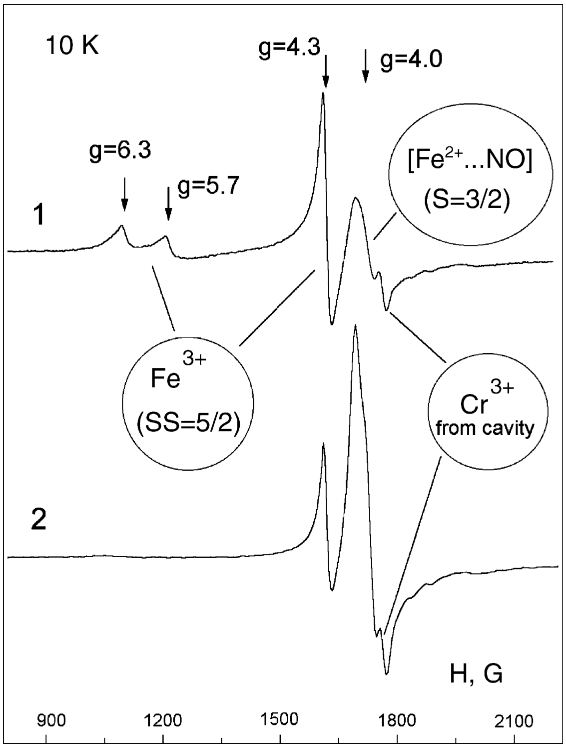

Fig. 4. EPR spectra of Fe-ZSM-5 dehydrated at 723 K (1) and 823 K (2) registered after NO adsorption at 293 K ($P = 10$ Torr) followed by brief evacuation at 173 K.

The splitting of the signal with $g_{\perp} = 6.0$ into two components symmetrical with respect to $g = 6.0$ is, most likely, due to weak rhombic distortion of the axial symmetry of the paramagnetic ion [34]. The disappearance of the EPR spectrum of these complexes observed experimentally after the zeolite evacuation at 823 K (Fig. 4, spectrum 2) is due to removal of hydroxyl ligands from the coordination sphere of Fe ions (reaction (7)).

In addition to the signals described above, a new EPR signal with $g = 4.0$ and a spectrum with $g_{\perp} = 1.99$, $g_{\parallel} = 1.86$, $A_Y = 31$ G typical for NO molecules adsorbed on Lewis acid sites of zeolites [35] can be distinguished in Fig. 4. Earlier [22] we have shown that the appearance of the signal with $g = 4.0$ after NO adsorption on Fe-ZSM-5 zeolites is due to the formation of iron–nitrosyl complexes with intermediate spin ($S = \frac{3}{2}$)

$$[\mathrm{Fe}^{2+}] + \mathrm{NO} \rightarrow [\mathrm{Fe}^{3+} \cdots \mathrm{NO}^{-}], \tag{9}$$

which implies a change of the spin state from $S = 2$ to $S = \frac{3}{2}$. Note that some Fe ions in the sample activated at 723 K exist as [$Fe^{3+}OH^{-}$] complexes (Fig. 4, spectrum 1). As a result, the concentration of [$Fe^{3+}\cdots NO^{-}$] complexes on this sample is lower than on the sample activated at 823 K (Fig. 4, spectrum 2). Thus, NO adsorption on Fe^{2+} ions leads to the change of their spin similar to their hydroxylation. The resulting nitrosyl complexes [$Fe^{3+}\cdots NO^{-}$] with $S = \frac{3}{2}$ are readily identified by EPR and can be used as paramagnetic probes for investigation of Fe^{2+} ions in oxide systems.

3.4.2. Low-spin ($S = \frac{1}{2}$) nitrosyl complexes

Different types of paramagnetic complexes with $S = \frac{1}{2}$ existing in equilibrium with the gas phase NO. These are stable in the temperature range of 100–250 K. Fig. 5 presents EPR spectra of such complexes observed under in situ conditions at 110 K. Spectrum 1 ($g_{av} = 1.97$, $\Delta H = 90$ G) is typical for monomeric NO stabilized on Lewis acid sites of the zeolite

$$[\mathrm{LAS}] + \mathrm{NO} \rightarrow [\mathrm{LAS} \cdots \mathrm{NO}]_{\mathrm{ads}}. \tag{10}$$

At low temperatures such complexes exhibit well-resolved EPR spectra (Fig. 4), whereas their spectra are broadened due to dynamic effects at 110 K known for other oxide systems [36]. The removal of the majority of adsorbed NO by evacuation at 173 K leads to disappearance of the corresponding EPR features.

New paramagnetic complexes with $g_{av} = 1.998$ and $\Delta H = 20$ G are observed in this case (Fig. 5, spectrum 2). Significant broadening of the EPR spectra up to 30 G when ^{57}Fe isotope is used and a clear dependence of the EPR signal intensity on the iron concentration in the samples unambiguously indicate that these spectra belong to iron–nitrosyl complexes in a low-spin state ($S = \frac{1}{2}$). The analysis of the formation conditions of these species and their stoichiometry indicate that, most likely, they contain three NO molecules. Interestingly, only the third weakly bound NO molecules accounts for the paramagnetism. The initial iron complexes and dinitrosyl complexes formed by addition of two NO molecules have zero spin and are not observed by EPR.

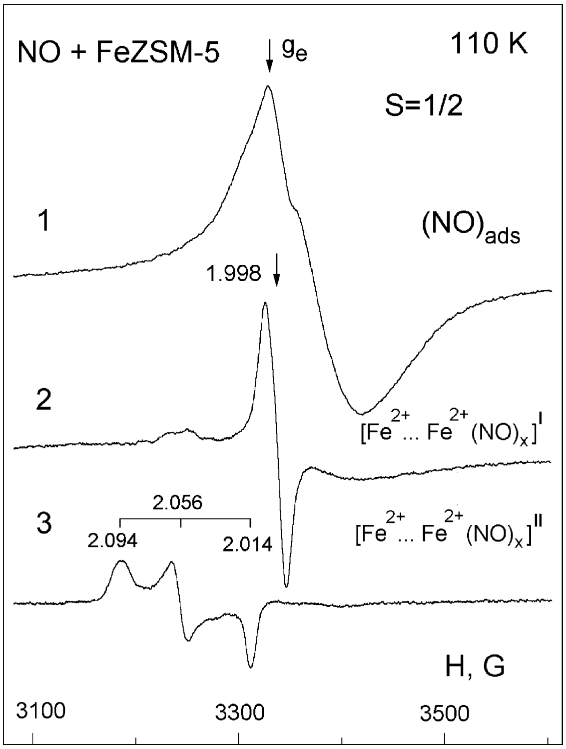

Fig. 5. EPR spectra of low-spin ($S = \frac{1}{2}$) complexes in Fe-ZSM-5 registered after NO adsorption at 293 K ($P = 10$ Torr) followed by 30 min evacuation at 113 K (1), 173 K (2) and 253 K (3).

The state of iron with $S = 0$ is not very common for oxide materials. This can be either monomeric Fe^{2+} ions in low-spin state or binuclear structures with two Fe ions bound antiferromagnetically ([Fe^{3+}–Fe^{3+}] or [Fe^{2+}–Fe^{2+}]). In comparison with oxygen anions, NO is a fairly strong ligand. Therefore, the preservation of the low-spin state after adsorption of three NO molecules on one Fe^{2+} ion appears to be rather unlikely. The existence of Fe^{2+} ions with three free coordination sites in a zeolite matrix is also very doubtful. In our opinion, such trinitrosyl complexes are formed on a binuclear Fe site

$$[\mathrm{Fe}^{2+}{-}\mathrm{Fe}^{2+}] + 2\mathrm{NO} \rightarrow [\mathrm{NO} \cdots \mathrm{Fe}^{2+}{-}\mathrm{Fe}^{2+} \cdots \mathrm{NO}] \tag{10a}$$

and

$$[\mathrm{NO}{-}\mathrm{Fe}^{2+}{-}\mathrm{Fe}^{2+}{-}\mathrm{NO}] + \mathrm{NO} \rightarrow [\mathrm{Fe}^{2+}{-}\mathrm{Fe}^{2+} \cdots (\mathrm{NO})_3], \tag{10b}$$

in which all species except the trinitrosyl have zero spin. The formation of a relatively strong dinitrosyl complex (reaction (10a)) does not alter the spin of the complex. Only the addition of the third NO molecule (reaction (10b)) leads to the appearance of paramagnetic complexes observable by EPR.

One more low-spin ($S = \frac{1}{2}$) iron–nitrosyl complex ($g_1 = 2.94$, $g_2 = 2.056$, $g_3 = 2.014$) similar to the one reported

Table 1
Parameters of EPR spectra and composition of paramagnetic complexes observed in Fe-ZSM zeolites

Observed EPR signal (g_1, g_2, g_3)	Spin and symmetry of the complex	Most likely composition of the complex	Designation of the active site and its spin
$g_{av} = 4.3$	$S = \frac{5}{2}$, $E/D = 1/3$	$[Fe^{3+}]$	Fe^{3+} (1, 2, 3)[a], $S = \frac{5}{2}$
6.3, 5.7, ($\sim g_e$)[b]	$S = \frac{5}{2}$, $E/D \ll 1$	$[Fe^{3+} \cdots OH^-]$	$[Fe^{2+}]$, $S = 2$
$g_\perp = 4.0$, ($g_\parallel \sim g_e$)[b]	$S = \frac{3}{2}$, $E/D \ll 1$	$[Fe^{3+} \cdots NO^-]$	$[Fe^{2+}]$, $S = 2$
$g_{av} = 1.998$, $\Delta H = 20$ G	$S = \frac{1}{2}$	$[(Fe^{2+})_2 \cdots (NO)_x]^{I}$	$[Fe^{2+} \cdots Fe^{2+}]^{I}$, $S = 0$
2.038, 2.058, 2.094	$S = \frac{1}{2}$	$[(Fe^{2+})_2 \cdots (NO)_x]^{II}$	$[Fe^{2+} \cdots Fe^{2+}]^{II}$, $S = 0$
$g_\perp = 1.99$, $g_\parallel = 1.86$, $A_y = 31$ G	$S = \frac{1}{2}$	$[NO \cdots A_s]$	A_s, $S = 0$
$g_{av} \sim g_e$, $\Delta H > 200$ G	$S \gg 1$	Oxide-like ferromagnetic nanoparticles	

[a] Earlier we have shown that, at least, three types of ions with such parameters of the EPR spectra with different localization and reactivity are present in the studied Fe-ZSM-5 zeolites [15].

[b] Expected g values of components not observed by EPR due to low intensity or overlapping with other lines are listed in parentheses.

earlier in literature [21,23] can be observed after evacuation at 253 K (Fig. 5, spectrum 3). The formation conditions and stoichiometry of these complexes are similar to the ones reported above. The main difference is much stronger bonding with NO providing stability of such complexes even after evacuation at 250 K.

3.5. Formation of α-oxygen and various iron-containing sites in Fe-ZSM-5

In summary, we wish to stress that a variety of iron-containing sites may be observed in Fe-ZSM-5 by EPR spectroscopy after careful selection of the experimental conditions and spin probes. Table 1 lists the magnetic resonance parameters as well the most likely composition of such paramagnetic complexes and the possible structure of such sites. The various sites have different chemical properties and account for different chemical reactions. Formation of α-oxygen by nitrous oxide decomposition on Fe-ZSM-5 zeolites is one of the few chemical reactions taking place on catalytic materials where the concentration of active sites can be measured relatively precisely. In this respect, it was of interest to establish a correlation between the concentrations of the various Fe sites as determined by EPR and sites accounting for α-oxygen stabilization determined by adsorption techniques.

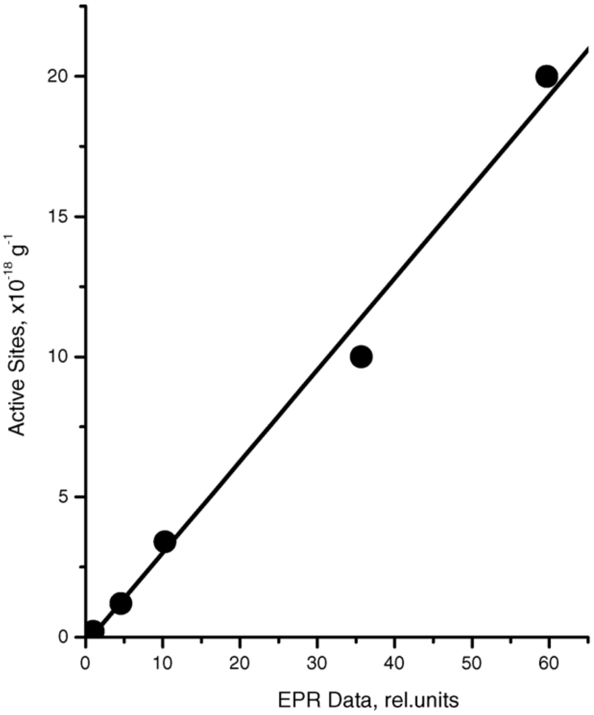

Fig. 6. Correlation between the concentrations of sites accounting for α-oxygen stabilization after N_2O decomposition measured by adsorption technique and paramagnetic complexes with $g_{av} = 1.998$ registered by EPR after NO adsorption over a series of Fe-ZSM-5 zeolites varying by Fe concentrations and synthesis methods.

To this end, a series of five samples with different concentrations of sites where α-oxygen could be stabilized was chosen for such experiments. Subsequently, the concentrations of various iron-containing sites discussed above ($[Fe^{3+}]$, $[Fe^{3+} \cdots NO^-]$, $[(Fe^{2+})_2 \cdots (NO)_x]^{I}$, $[(Fe^{2+})_2 \cdots (NO)_x]^{II}$ complexes) were estimated under optimal conditions as determined in this contribution. These experiments produced a fairly unexpected result (Fig. 6). A good correlation with the concentration of sites accounting for α-oxygen stabilization was observed only for the signal with $g_{av} = 1.998$ belonging to $[(Fe^{2+})_2 \cdots (NO)_x]^{I}$ associated with binuclear iron sites ($[Fe^{2+} \cdots Fe^{2+}]^{I}$ with $S = 0$). Further studies exploring the role of the observed correlation for catalytic nitrous oxide decomposition and benzene oxidation and the structure of these sites are in our immediate plans.

4. Conclusions

In this study we have shown new approaches to characterize Fe species in zeolitic catalysts by alteration of their spin state by adsorption of gaseous probe molecules akin to the investigation of EPR-silent iron structures in enzymes and other biological objects. Complexes of Fe ions with half-integer spin ($S = \frac{1}{2}$, $S = \frac{3}{2}$ and $S = \frac{5}{2}$) are reliably identified by EPR. This not only allows to make Fe^{2+} species amenable to EPR observation but also $[Fe^{3+}O^-]$ complexes formed upon decomposition of nitrous oxide. The observed correlation between the concentrations of sites active in N_2O decomposition at low temperatures (α-sites) and low-spin ($S = \frac{1}{2}$) iron–nitrosyl complexes formed after NO adsorption appears to a good starting point for the further development of studies aimed at understanding the nature of the active sites and the mechanism of their action. Undoubtedly, the results reported in this paper require additional independent verification. Nevertheless, the suggested approaches to investigation of iron-containing active sites by EPR are fairly universal and can be applied to many other oxide systems, especially systems with low Fe concentration.

Acknowledgements

Financial support of the Russian Foundation for Basic Research (Grant 03-03-33178) and the Dutch Science Foundation (Grant 047-015-001-NWO) is acknowledged with gratitude. AMV and GMZ are grateful to the Russian Federation Program for Science Schools support (Project 1140.2003.3).

References

[1] G.I. Panov, G.A. Sheveleva, A.S. Kharitonov, V.N. Romannikov, L.A. Vostrikova, Appl. Catal. A 82 (1992) 31.

[2] G.I. Panov, A.K. Uriarte, M.A. Rodkin, V.I. Sobolev, Catal. Today 41 (1998) 365.

[3] R. Joyner, M. Stockenhuber, J. Phys. Chem. B 103 (1999) 5963.

[4] A. Ribera, I.W.C.E. Arends, S. de Vries, J. Perez-Ramirez, R.A. Sheldon, J. Catal. 195 (2000) 287.

[5] G. Berlier, G. Spoto, S. Bordiga, G. Ricchiardi, P. Fisicaro, A. Zecchina, I. Rossetti, E. Selli, L. Forni, E. Giamello, C. Lamberti, J. Catal. 208 (2002) 64.

[6] E.J.M. Hensen, Q. Zhu, R.A. van Santen, J. Catal. 220 (2003) 260.

[7] J. Perez-Ramirez, F. Kapteijn, J.C. Groen, A. Domenech, G. Mul, J.A. Moulijn, J. Catal. 214 (2003) 33.

[8] L. Kiwi-Minsker, D.A. Bulushev, A. Renken, J. Catal. 219 (2003) 273.

[9] G.D. Pirngruber, J. Catal. 219 (2003) 456.

[10] V.I. Sobolev, A.S. Kharitonov, Y.A. Paukshtis, G.I. Panov, J. Mol. Catal. 84 (1993) 117.

[11] K.A. Dubkov, V.I. Sobolev, E.P. Talsi, M.A. Rodkin, N.H. Watkins, A.A. Shteinman, G.I. Panov, J. Mol. Catal. 123 (1997) 155.

[12] K.A. Dubkov, N.S. Ovanesyan, A.A. Shteinman, E.V. Starokon, G.I. Panov, J. Catal. 207 (2002) 341.

[13] L.M. Kustov, V.B. Kazansky, P. Ratnasamy, Zeolites 7 (1987) 79.

[14] A.V. Kucherov, A.A. Slinkin, Zeolites 8 (1988) 110.

[15] A.M. Volodin, V.I. Sobolev, G.M. Zhidomirov, Kinet. Catal. 39 (1998) 775.

[16] J.R. Galpin, G.A. Veldink, J.F.G. Vliegenthart, J. Boldingh, Biochim. Biophys. Acta 536 (1978) 356.

[17] J.C. Salerno, J.N. Siedow, Biochim. Biophys. Acta 579 (1979) 246.

[18] Y. Zhang, M.A. Pavlosky, C.A. Brown, T.E. Westre, B. Hedman, K.O. Hodson, E.I. Solomon, J. Am. Chem. Soc. 114 (1992) 9189.

[19] N.E. Le Brun, M.R. Cheesman, A.J. Thomson, G.R. Moore, S.C. Andrews, J.R. Guest, P.M. Harrison, FEBS Lett. 323 (1993) 261.

[20] M. Lee, P. Arosio, A. Cozzi, N.D. Chasteen, Biochemistry 33 (1994) 3679.

[21] J.W. Jermyn, T.J. Johnson, E.F. Vansant, J.H. Lunsford, J. Phys. Chem. 77 (1973) 2964.

[22] A.M. Volodin, K.A. Dubkov, A. Lund, Chem. Phys. Lett. 333 (2001) 41.

[23] P. Fisicaro, E. Giamello, G. Berlier, C. Lamberti, Res. Chem. Intermed. 29 (2003) 805.

[24] V.A. Bolshov, A.M. Volodin, G.M. Zhidomirov, A.A. Shubin, A.F. Bedilo, J. Phys. Chem. 98 (1994) 7551.

[25] I. Zilberberg, R.W. Gora, G.M. Zhidomirov, J. Leszczynski, J. Chem. Phys. 117 (2002) 7153.

[26] J. Jia, Q. Sun, B. Wen, L.X. Chen, W.M.H. Sachtler, Catal. Lett. 82 (2002) 7.

[27] M. Che, A.J. Tench, Adv. Catal. 31 (1982) 77.

[28] A. Volodin, Catal. Today 58 (2000) 103.

[29] Y. Ben Taarit, M.C.R. Symons, A.J. Tench, J. Chem. Soc. Farad. Trans. I 73 (1977) 1149.

[30] N.I. Lipatkina, V.A. Shvets, V.B. Kazansky, Kinet. Katal. 19 (1978) 979.

[31] A.M. Volodin, A.E. Cherkashin, React. Kinet. Catal. Lett. 18 (1981) 243.

[32] K.A. Dubkov, E.V. Starokon, E.A. Paukschtis, A.M. Volodin, G.I. Panov, Kinet. Katal. 45 (2004) 218.

[33] K.A. Dubkov, E.A. Paukschtis, G.I. Panov, Kinet. Katal. 42 (2001) 230.

[34] W.R. Hagen, Adv. Inorg. Chem. 38 (1992) 165.

[35] P.H. Kasai, R.M. Gaura, J. Phys. Chem. 86 (1982) 4257.

[36] A. Volodin, D. Biglino, Y. Itagaki, M. Shiotani, A. Lund, Chem. Phys. Lett. 327 (2000) 165.